



Analysis of the {4-Nicotinamido-4-Oxo-2-Butenoic Acid's} Electrochemical Polymerization as an Anti-Corrosion Layer on Stainless-Steel Alloys

Zahra Al-Timimi^{1*}, Zeina J Tammemi²

¹Laser Physics Department, College of Science for Women,
University of Babylon, Hillah, 51001, IRAQ

²College of Dentistry,
University of Babylon, Hillah, 51001, IRAQ

*Corresponding Author

DOI: <https://doi.org/10.30880/jsmpm.2022.02.02.001>

Received 25 May 2022; Accepted 05 September 2022; Available online 31 October 2022

Abstract: The {Poly4-Nicotinamido-4-Oxo-2-Butenoic Acid's}, which serves as an anti-corrosion layer, was produced by electropolymerized the {4-Nicotinamido-4-Oxo-2-Butenoic Acid's} monomer onto 316-grade steel material. The produced polymer's structure and characteristics were evaluated using SEM, cyclic voltammetry, and other techniques. The corrosion resistance of stainless steel, both uncoated and coated in a corrosive medium of 0.2M HCl solution was examined using an electrochemical polarisation technique at temperatures ranging from (293-323) K. Nanomaterials such as nano zinc oxide and graphene were introduced to monomer solutions at various concentrations to increase the corrosion resistance of stainless-steel surfaces. According to the findings, adding nano components to a polymeric coating increased its protective effectiveness. Thermodynamic and kinetic activation properties were also investigated. The percentage of protection efficiencies and polarisation resistance values of the covering polymer decreased as the temperature rose. As the temperature climbed, the corrosion current density increased, although the corrosion potential decreased. In SEM and AFM experiments, the development of a protective coating on the surface of 316-grade stainless steel was demonstrated to protect it.

Keywords: Nanomaterials, stainless steel, nicotinamide, coating

1. Introduction

Despite substantial advances in corrosion prevention and control sciences and technologies, corrosion, particularly of metals and alloys, remains a major source of concern for many industries across the world. Corrosion can be avoided in most cases by making suitable adjustments to the environment, such as adding inhibitors or choosing corrosion-resistant materials, as well as material surfaces, such as coatings and films [1,2]. Stainless steel is a widely used material in a range of industries, and it's an excellent choice for corrosion resistance. Corrosion resistance in steel material is associated with the development of a thin passive layer on the surface of materials. Extreme chloride conditions may compromise the natural thinner layer's endurance, leading to isolated corrosion potential as well as irreversible damage [3,4].

The ability to resist corrosion attack is attributed to the presence of a thin protective covering made of chromium-enriched oxide in aqueous conditions. However, the steel experiences cracking corrosion in chloride-containing environments. This targeted attack severely restricts the material's use for biological applications. Ions including iron,

*Corresponding author: dr.altimimizahra@gmail.com

chromium, as well as nickel that are discharged into the biological environment around the alloy decrease biocompatibility[5,6].

Several technologies have been applied to make stainless surfaces that are more protective, such as the application of conjugated polymers. Due to a variety of benefits, such as ease of synthesis, high stability, and excellent biocompatibility in biosensors, {Poly4-Nicotinamido-4-Oxo-2-Butenoic Acid's} is a desirable substitute for protecting stainless [7].

In recent years, there has been a significant amount of interest in the utilization of conjugated polymers to prevent corrosion. Both aqueous and organic liquids can be converted into conducting polymers through electrical or chemical polymerization. The electrochemical approach is popular because it allows for greater control over film thickness and morphology by adjusting a number of factors, including initial concentration, pH, monomers concentration, as well as the constitution of the liquid electrolyte. Polymer insulation materials are good alternatives for protecting metal because of their conductivity qualities. A few examples of applications include sensors, chargers, small molecule electronics, membrane technology separation, photovoltaic panels, as well as storage systems for energy [8,9].

In this investigation, the monomer was electro polymerized on a stainless surface to create the polymeric film. The copolymer film was evaluated using cyclic voltammetry, AFM, as well as SEM. Using the electrochemical measurements technique, corrosion investigations on untreated and coated stainless in 0.2 M of HCl at temperatures of (293-323) K have been conducted. The effects of adding nanoscale materials like graphene and nanoparticles to a polymerization method to produce an anti-corrosion covering had been investigated.

2. Materials and Methods

2.1 Synthesize of the {4-Nicotinamido-4-Oxo-2-Butenoic Acid's} Monomer

To produce {4-nicotinamide-4-oxo-2-butenoic acid}, the following procedure was employed. In 20 ml of dioxane (C₄H₈O₂), maleic anhydride (C₂H₂(CO)₂O) (1g, 0.01mol) was dissolved. A combination was given (1g, 0.01 mol) of nicotinamide (C₆H₆N₂O) and allowed to sit at room temperature for 6 hours. Under vacuum, a dark yellow precipitate had been produced, filtered, and dried.

2.2 Electro Polymerization of the {4-Nicotinamido-4-Oxo-2-Butenoic Acid's} Monomer

A standard (DC) power supply electro polymerized the monomer on the 316-grade stainless steel surface (anodic electrode) (Galvanostatic method). Electrodes were rinsed and dried after being washed with deionized H₂O and (CH₃)₂CO; for preparing the polymerization solution, a dissolve of 0.1g of monomer in a 100ml of H₂O and a few drops of H₂SO₄ as a supporting electrolyte. At room temperature, the polymeric coating was applied to the anodic electrode. After the monomer solution was distributed, a 0.004 g of graphene was added, followed by 0.04 g of Nano-ZnO to produce the corrosion-resistant polymeric covering [10,11].

For the effectiveness of this regard reaction that produced the synthetic polymer film layer on the surface of the metal as well as allowed for grafting, a cationic mechanism was suggested. In the first stage, the electron was transferred first from the monomer to the surface of the metal, serving as the working electrode. The electrode surface becomes positively charged as a result of the cation radical that forms as a result of this electron transfer and adsorbs there. A component with a low molecular weight is produced as a result of the cation radical desorbing and interacting in solution. The charging end of the immobilized oxidized monomer is added by a cationic technique towards the charging end of the monomer molecule [12,13].

2.3 Measurement of Electrochemical Corrosion

To measure corrosion, three types of electrodes were used: a saturated calomel electrode, a stainless-steel electrode, and an auxiliary electrode. Anodic and cathodic polarization for corrosion was done under potentiates conditions in 0.2 M of HCl at (293-323) K. The following equation was used to compute the value of protection efficiencies (PE%) [14]. The density current values for untreated and coated stainless steel are *i*_{ocorr} and *i*_{corr}, respectively.

$$PE\% = \left[1 - \frac{(i_{corr})_{coated}}{(i_{ocorr})_{uncoated}} \right] * 100 \quad (1)$$

The following Stern-Geary equation was used to compute the polarization resistance (R_p) [15]:

$$R_p = \frac{B_a * B_c}{2.303(B_a + B_c) i_{corr}} \quad (2)$$

The effects of temperature on corrosion rate in 0.2M HCl solution were explored using the Arrhenius equation [16].

$$i_{corr} = Ae^{\left(\frac{-Ea}{RT}\right)} \quad (3)$$

Equation (3) was logarithmically transformed as follows:

$$\text{Log } i_{corr} = \text{Log } A - \frac{Ea}{2.303 RT} \quad (4)$$

The equation for the transition state was written as follows[16]:

$$\text{Log } \frac{i_{corr}}{T} = \text{Log} \left[\frac{R}{Nh} + \frac{\Delta S^*}{2.303 R} \right] - \frac{\Delta H^*}{2.303 RT} \quad (5)$$

Using the following equation, the activation Gibbs free energy (ΔG^*) was obtained [17,18]:

$$\Delta G^* = \Delta H^* - T\Delta S^* \quad (6)$$

2.4 Electrodeposition of Polymeric Film

To deposit a polymeric film on a stainless-steel electrode, cyclic voltammetry was used to electro polymerize an aqueous solution of (0.2g) monomer; (200ml) H₂O, and drops H₂SO₄ across a range of (-2000 to 2000) mV with scan rate of 40 mV/s.

3. Results and Discussion

3.1 Cyclic Voltammetry

A cyclic voltammogram was employed to record the electrodeposition of the polymeric layer on stainless steel. It was utilized to investigate the polymeric film's redox characteristics. At first scan, the oxidation wave appears to start at 1.8V, indicating that the monomer has been oxidized. The intensity of this oxidation wave decreased in succeeding scans, while oxidation wave was changed to a greater potential, which could indicate that the monomer was electropolymerized. In subsequent scans, the oxidation wave's intensity fell while its potential increased, possibly indicating that the monomer had undergone electro polymerization. The rates of polymerization accelerated above 1.8 V in potential. A green polymeric layer materialized at the conclusion of each cycle. An increase in anodic currents was seen in conjunction with the electro polymerization of the polymer, albeit these currents gradually dropped as the number of scans increased. As a result, as the number of cycles increased, the current decreased as the coating film expanded during the cyclical process [19,20].

3.2 Tests for Corrosion

The corrosion of a polymeric film-coated surface was investigated using electrochemical polarization. Fig. 1 shows polarization curves for uncoated and coated stainless steel by the polymeric film with and without nanomaterial in 0.2 HCl solutions at (293-323) K. Extrapolating cathodic and anodic lines to a junction site produced (E_{corr}) propensity for corrosion, and (i_{corr}) current density of corrosion. (β_c) in addition (β_a) cathodic, anodic Tafel slopes have been determined using the same Fig. 1. Table 1 displays corrosion parameter data, which includes the following: E_{corr} (mV); i_{corr} ($\mu\text{A}/\text{cm}^2$); β_a also β_c in (mV/Dec); weight loss (W.L) in ($\text{g}/\text{m}^2\text{d}$); penetration loss (P.L) in (mm/y); R_p (Ω/cm^2), R_p ; and PE%.

The data reveal that E_{corr} and i_{corr} increased as the temperature rose. E_{corr} switched to more active (cathodic) values as the temperature rose. The i_{corr} of the coated stainless was significantly lower than that of the untreated stainless after adding the nanomaterial. Furthermore, as demonstrated in the plots, the E_{corr} for the coated stainless had been pushed towards an advanced location when compared to the untreated stainless. That means the corrosion protection is also anodic protection. Additionally, the R_p values grew more in the treated than in the untreated stainless steel, specifically when the nanomaterials have been introduced [21,22].

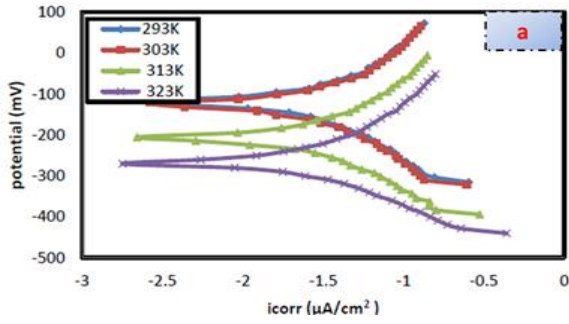


Fig. 1(a) - Polarization curves for uncoated stainless-steel corrosion in (0.2M) HCl at changed temperatures

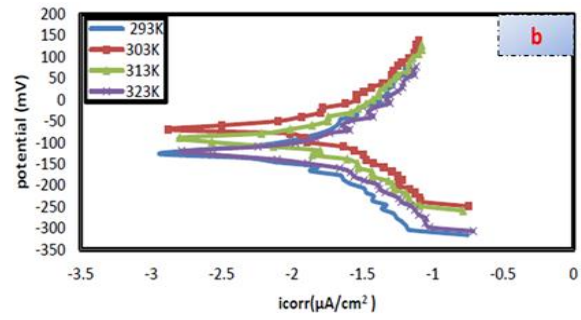


Fig. 1(b) - At different temperatures, polarization curves pro the corrosion of treated stainless-steel

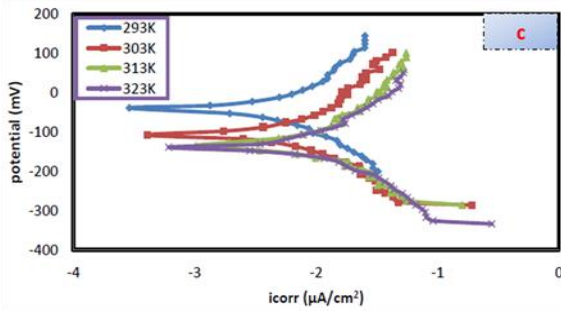


Fig. 1(c) - At various temperatures, polarization curves for corrosion of coated 316-grade stainless steel with polymeric film modified with graphene in (0.2M) HCl

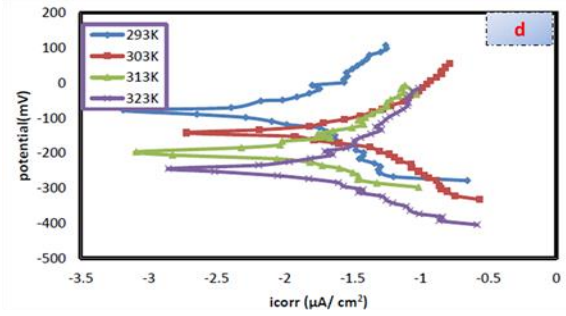


Fig. 1(d) - At various temperatures, polarization curves for corrosion of coated stainless steel with polymeric film modified with Nano ZnO in (0.2M) HCl

Table 1 - Corrosion characteristics of the un-coated and coated stainless steel

Covering (Coating)	Absolute temperature (K)	Ecorr	Icorr	β_c	β_a	W.L	P.L	PE%	Rp
Uncoated stainless steel	293	116.7	18.42	188.7	159.8	1.48	$2.00 \cdot 10^{-1}$	-	2039.681
	303	126.0	21.37	199.1	185.8	1.72	$2.32 \cdot 10^{-1}$	-	1952.858
	313	206.6	24.35	207.7	220.5	1.96	$2.65 \cdot 10^{-1}$	-	1906.821
	323	271.8	25.89	171.6	258.5	2.08	$2.82 \cdot 10^{-1}$	-	1729.746
Coated stainless steel with polymeric film	293	63.8	4.67	74.4	94.0	$3.76 \cdot 10^{-1}$	$5.08 \cdot 10^{-1}$	74.65	3861.427
	303	67.8	5.65	77.0	94.5	$4.55 \cdot 10^{-1}$	$6.15 \cdot 10^{-1}$	73.56	3260.739
	313	88.1	8.61	131.0	128.9	$6.93 \cdot 10^{-1}$	$9.36 \cdot 10^{-1}$	64.64	3276.581
	323	122.4	10.39	136.6	170.2	$8.36 \cdot 10^{-1}$	$1.13 \cdot 10^{-1}$	59.87	3166.981
Coated stainless steel with polymeric film modified with graphene	293	39.9	1.83	75.6	69.9	$1.48 \cdot 10^{-1}$	$2.00 \cdot 10^{-1}$	90.00	8617.692
	303	107.8	2.99	87.5	103.5	$2.40 \cdot 10^{-1}$	$3.25 \cdot 10^{-1}$	86.00	6885.729
	313	135.3	3.76	69.6	89.8	$3.02 \cdot 10^{-1}$	$4.09 \cdot 10^{-1}$	84.55	4528.094
	323	140.6	6.89	111.2	178.7	$5.54 \cdot 10^{-1}$	$7.49 \cdot 10^{-1}$	73.39	4319.843
Coated stainless steel with polymeric film modified with Nano ZnO	293	79.4	3.09	73.9	68.9	$2.49 \cdot 10^{-1}$	$3.36 \cdot 10^{-1}$	83.22	5010.523
	303	142.3	5.25	48.5	50.5	$4.22 \cdot 10^{-1}$	$5.71 \cdot 10^{-1}$	75.40	2046.184
	313	195.6	5.93	84.7	95.1	$4.77 \cdot 10^{-1}$	$6.45 \cdot 10^{-1}$	75.64	3280.391
	323	245.8	7.97	100.7	111.9	$6.41 \cdot 10^{-1}$	$8.67 \cdot 10^{-1}$	69.22	2887.647

3.3 Thermodynamics and Kinetics

Arrhenius graphs for corrosion of the coated as well as un-coated stainless steel are shown in Fig. 2 (a) and Fig. 2 (b). Inside Fig. 2 are plots of $\log(i_{corr}/T)$ vs. $(1/T)$. The slopes and intercepts were used to determine (ΔH^*) and (ΔS^*) , respectively.

- Δ - uncoated stainless steel
- \square - coated stainless steel with polymeric film
- Δ - coated stainless steel with polymeric film modified with graphene
- \times - coated stainless steel with polymeric film modified with ZnO

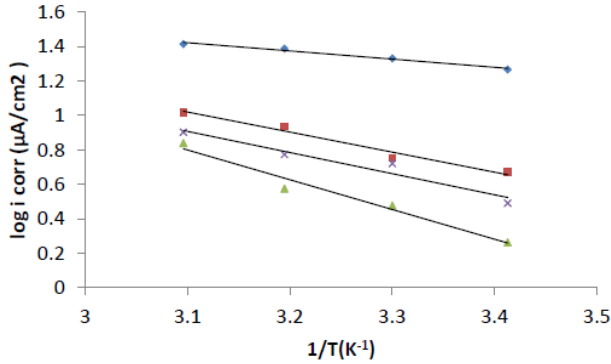


Fig. 2(a) - The plot of $\log i_{corr}$ opposed to $1/T$ for uncoated and coated stainless steel with polymeric film with and without nanomaterials

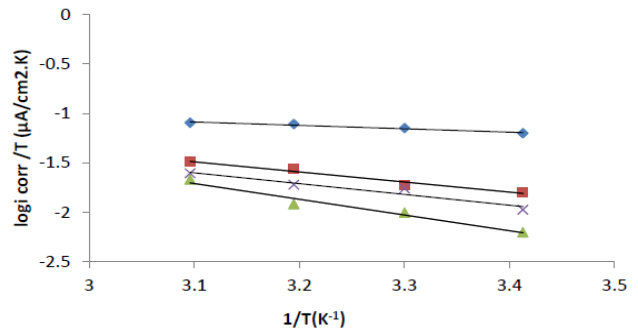


Fig. 2(b) - The plot $\log(i_{corr}/T)$ Vs. $(1/T)$ of uncoated, coated stainless steel with polymeric film with and without nanomaterials

Table 2 lists all of the kinetics parameters, including thermodynamics. The inclusion of polymeric film increased activation energies, indicating that the coating has a stronger protective efficiency. Activation energies have increased as a result of the addition of different nanomaterials, indicating a rise in the energy barrier [23]. The positive activation enthalpies imply that the stainless steel transition state process is endothermic [24].

Table 2 - Thermodynamic parameters of the transition state for corrosion of stainless steel un-coated and coated by polymeric film in absence, presence of nanomaterials at various temperatures

Covering (Coating)	Absolute temperature (K)	ΔG^*	ΔH^*	$-\Delta S^*$	R^2	E_a	A	R^2
Uncoated stainless steel	293	64.593	6.546	198.112	0.958	9.103	4.721×10^{26}	0.979
	303	66.574						
	313	68.555						
	323	70.536						
Coated stainless steel with polymeric film	293	68.049	19.624	165.276	0.966	22.180	2.449×10^{28}	0.973
	303	69.703						
	313	71.355						
	323	73.008						
Coated stainless steel with polymeric film modified with graphene	293	70.277	30.471	135.858	0.965	33.027	8.421×10^{29}	0.969
	303	71.636						
	313	72.995						
	323	74.353						
Coated stainless steel with polymeric film modified with Nano ZnO	293	68.794	20.879	163.528	0.929	23.426	3.022×10^{28}	0.944
	303	70.429						
	313	72.064						
	323	73.699						

3.4 Atomic Force Microscopy (AFM)

Fig. 3 depicts 2D, 3D AFM images for all coating films that have been applied. The most extensively used metrics in AFM analysis to evaluate surface roughness are mean grain size (M.G.S), root mean squares (R.M.S), in addition the roughness average (Ra). A list of these parameters can be found in Table 3. The results show that after using nanomaterials to modify polymeric films, the surface roughness of all coated films was reduced due to the smaller grain size. As a result, the lower the surface roughness, the better the coating's barrier effect for preventing corrosion [25,26].

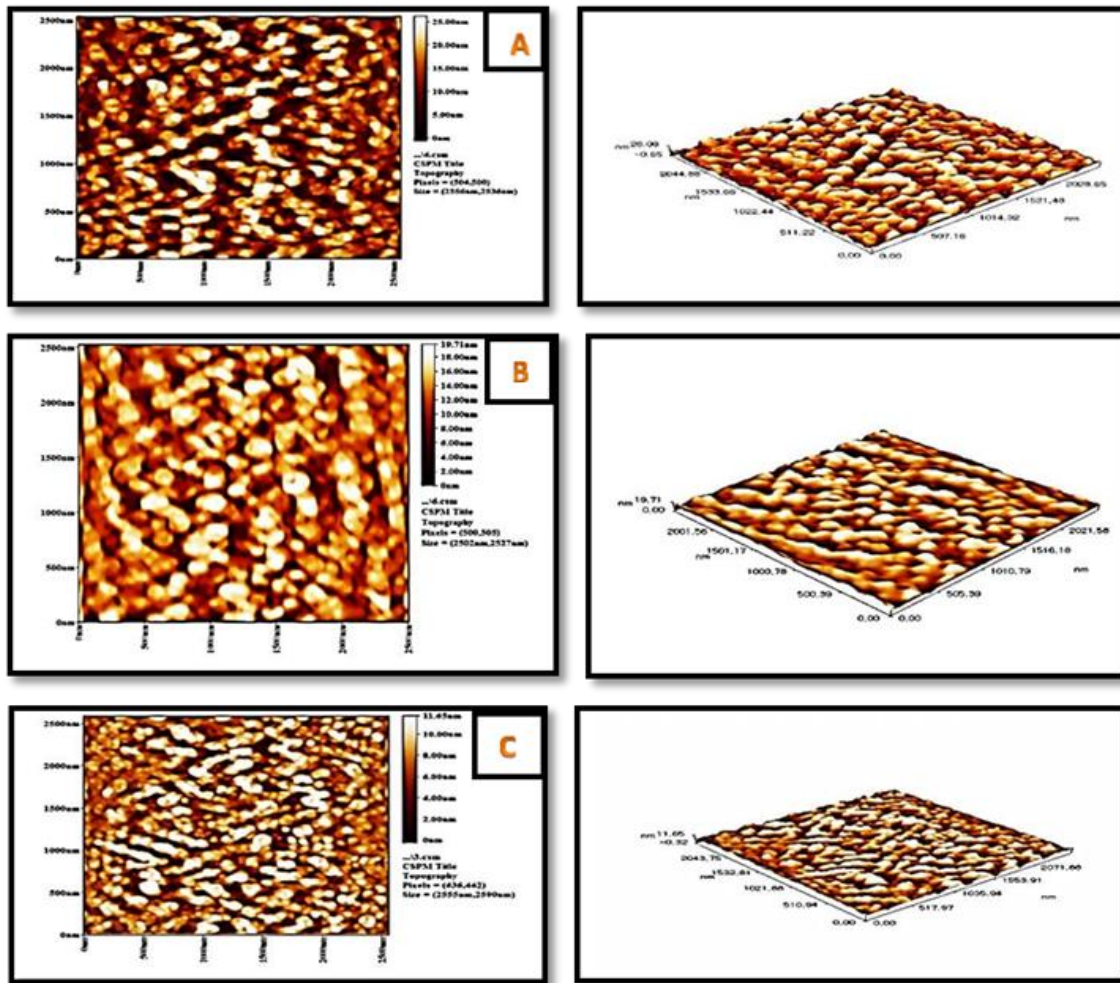


Fig. 3 - AFM images of; (a) polymeric film; (b) polymeric film adapted by Nano graphene; (c) polymeric film adapted by Nano ZnO

Table 3 - Values for M.G.S, R.M.S and Ra

Layer	M.G.S (nm)	R.M.S (nm)	Ra (nm)
Layered stainless steel by polymeric film	95.61	5.25	4.24
Layered stainless steel with polymeric film modified by graphene	93.41	3.02	2.42
Layered 316-grade stainless steel with polymeric film adapted by Nano ZnO	87.06	2.01	1.58

3.5 Scanning Electron Microscopy (SEM)

On the surface of stainless steel, the polymeric film has a heterogeneous distribution with some pores, whereas the polymeric film adapted by Nano graphene showed combinations of sphere-shaped grains of various dimensions, and the polymeric film adapted by Nano ZnO showed a homogeneous spreading on the surface of stainless steel with fibril structure Fig. 4. (A-C). It was demonstrated that applying a protective coating to the surface of 316-grade stainless steel protects it [25,26].

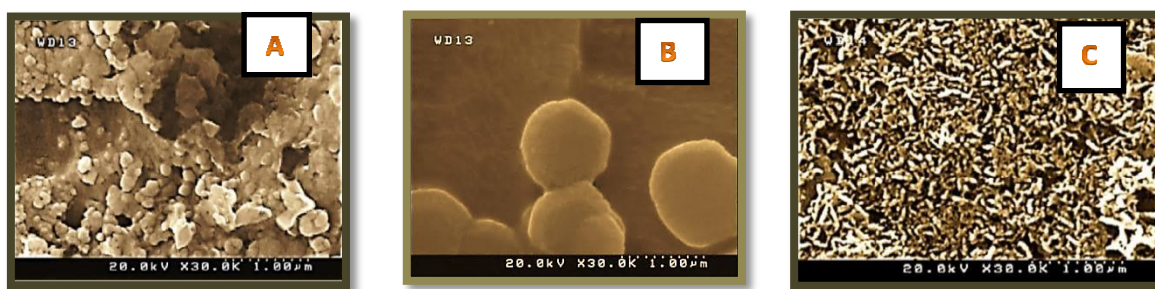


Fig. 4 - SEM images; (a) polymeric film; (b) polymeric film modified with Nano graphene; (c) polymeric film modified with Nano ZnO

4. Conclusions

On 316-grade stainless steel, monomer electro polymerization provided a good anti-corrosion coating. The percentage of protection efficiencies and polarisation resistance values of the covering polymer decreased as the temperature rose. The protection efficiencies percent value improved after the nanomaterial, notable graphene, was introduced. As the temperature climbed, the corrosion current density increased, although the corrosion potential decreased. The course of corrosion had been changed to one that provided anodic protection. SEM and AFM investigations have demonstrated that the creation of a protective layer on the surface of 316-grade stainless would safeguard it.

Acknowledgement

The authors are grateful to the University of Babylon for providing academic, moral, and laser laboratory support. Thank you to the entire technical staff at the Women's Science Colleges Laser Department.

References

- [1] Los', I.S., Rozen, A.E., Dub, A.V., Korneev, A.E., Kireev, S.Y., Kharina, I.L., & Safonov, I.A. (2020). Regularities of creation of layered metal corrosion-resistant materials with internal protector. *Izv Volgogr STATE Tech Univ*, pp. 24–30
- [2] Zhang, Y., Zuo, T.T., Tang, Z., Gao, M.C., Dahmen, K.A., Liaw, P.K., & Lu, Z.P. (2014). Microstructures and properties of high-entropy alloys. *Progress in Materials Science*, 61, 1-93.
- [3] Lo, K.H., Shek, C.H., & Lai, J.K.L. (2009). Recent developments in stainless steels. *Materials Science and Engineering: R: Reports*, 65(4-6), 39-104.
- [4] Ko, G., Kim, W., Kwon, K., & Lee, T.K. (2021). The corrosion of stainless steel made by additive manufacturing: A review. *Metals*, 11(3), 516.
- [5] Huang, C., Qian, X., & Yang, R. (2018). Thermal conductivity of polymers and polymer nanocomposites. *Materials Science and Engineering: R: Reports*, 132, 1-22.
- [6] Chobaomsup, V., Metzner, M., & Boonyongmaneerat, Y. (2020). Superhydrophobic surface modification for corrosion protection of metals and alloys. *Journal of Coatings Technology and Research*, 17(3), 583-595.
- [7] Zhang, Y., Zhang, D., Wei, X., Zhong, S., & Wang, J. (2018). Enhanced tribological properties of polymer composite coating containing graphene at room and elevated temperatures. *Coatings*, 8(3), 91.
- [8] Ren, Y., Zhang, L., Xie, G., Li, Z., Chen, H., Gong, H., Xu, W., Guo, D., & Luo, J. (2021). A review on tribology of polymer composite coatings. *Friction*, 9(3), 429-470.
- [9] Abushrida, A., Elhuni, I., Taresco, V., Marciani, L., Stolnik, S., & Garnett, M.C. (2020). A simple and efficient method for polymer coating of iron oxide nanoparticles. *Journal of Drug Delivery Science and Technology*, 55, 101460.
- [10] Roselli, M., Finamore, A., Garaguso, I., Britti, M.S., & Mengheri, E. (2003). Zinc oxide protects cultured enterocytes from the damage induced by Escherichia coli. *The Journal of Nutrition*, 133(12), 4077-4082.
- [11] Shayeh, J.S., Ehsani, A., Ganjali, M.R., Norouzi, P., & Jaleh, B.J.A.S.S. (2015). Conductive polymer/reduced graphene oxide/Au nano particles as efficient composite materials in electrochemical supercapacitors. *Applied Surface Science*, 353, 594-599.
- [12] Timimi, Z., & Tammemi, Z.J. (2022). Polymer Blends and Nanocomposite Materials Based on Polymethyl Methacrylate (PMMA) for Bone Regeneration and Repair: Characterization and Preparation. *Journal of Sustainable Materials Processing and Management*, 2(1), 15-23.
- [13] Henry, C.R. (2005). Morphology of supported nanoparticles. *Progress in Surface Science*, 80(3-4), 92-116.

- [14] Forouzandeh, P., Kumaravel, V., & Pillai, S.C. (2020). Electrode materials for supercapacitors: a review of recent advances. *Catalysts*, 10(9), 969.
- [15] Wu, Z., Li, L., Yan, J.M., & Zhang, X.B. (2017). Materials design and system construction for conventional and new-concept supercapacitors. *Advanced science*, 4(6), 1600382.
- [16] Bentiss, F., Lebrini, M., & Lagrenée, M. (2005). Thermodynamic characterization of metal dissolution and inhibitor adsorption processes in mild steel/2, 5-bis (n-thienyl)-1, 3, 4-thiadiazoles/hydrochloric acid system. *Corrosion Science*, 47(12), 2915-2931.
- [17] Lorenzetti, M., Pellicer, E., Sort, J., Baró, M.D., Kovač, J., Novak, S., & Kobe, S. (2014). Improvement to the corrosion resistance of Ti-based implants using hydrothermally synthesized nanostructured anatase coatings. *Materials*, 7(1), 180-194.
- [18] Farag, A.A. (2020). Applications of nanomaterials in corrosion protection coatings and inhibitors. *Corrosion Reviews*, 38(1), 67-86.
- [19] Pourhashem, S., Saba, F., Duan, J., Rashidi, A., Guan, F., Nezhad, E.G., & Hou, B. (2020). Polymer/Inorganic nanocomposite coatings with superior corrosion protection performance: A review. *Journal of Industrial and Engineering Chemistry*, 88, 29-57.
- [20] Al-Timimi, Z., & Tammemi, Z.J. (2022). Utilizing nanomagnetic materials to eliminate Pb²⁺ and Cd²⁺ from aqueous mixtures. *Current Research in Green and Sustainable Chemistry*, 5, 100290.
- [21] Joseph, B., John, S., Joseph, A., & Narayana, B. (2010). Imidazolidine-2-thione as corrosion inhibitor for mild steel in hydrochloric acid. *Indian Journal of Chemical Technology*, 17, 366–374.
- [22] Mobin, M., Zehra, S., & Parveen, M. (2016). L-Cysteine as corrosion inhibitor for mild steel in 1 M HCl and synergistic effect of anionic, cationic and non-ionic surfactants. *Journal of Molecular Liquids*, 216, 598-607.
- [23] Noor, E.A., & Al-Moubaraki, A.H. (2008). Thermodynamic study of metal corrosion and inhibitor adsorption processes in mild steel/1-methyl-4 [4'(-X)-styryl pyridinium iodides/hydrochloric acid systems. *Materials Chemistry and Physics*, 110(1), 145-154.
- [24] Labouche, D., & Parrott, B. (2010). Contribution of nanomaterials to high corrosion protection. *Transactions of the Institute of Metal Finishing*, 88(1), 8-10.
- [25] Zhu, Q., Li, E., Liu, X., Song, W., Zhao, M., Zi, L., Wang, X., & Liu, C. (2020). Synergistic effect of polypyrrole functionalized graphene oxide and zinc phosphate for enhanced anticorrosion performance of epoxy coatings. *Composites Part A: Applied Science and Manufacturing*, 130, 105752.
- [26] Karthikeyan, P., Malathy, M., & Rajavel, R. (2017). Poly (ophenylenediaminecoaniline)/ZnO coated on passivated low nickel stainless steel. *Journal of Science: Advanced Materials and Devices*, 2(1), 86-92.
- [27] Kausar, A. (2019). Corrosion prevention prospects of polymeric nanocomposites: A review. *Journal of Plastic Film & Sheeting*, 35(2), 181-202.